



ELSEVIER

Nanomedicine: Nanotechnology, Biology, and Medicine
xx (xxxx) xxx

nanomedjournal.com

The impact of size and charge on the pulmonary pharmacokinetics and immunological response of the lungs to PLGA nanoparticles after intratracheal administration to rats

Shadabul Haque, PhD^{a,b}, Colin W. Pouton, PhD^a, Michelle P. McIntosh, PhD^a,
David B Ascher, PhD^c, David W Keizer, PhD^c, Michael Whittaker, PhD^{a,b,*},
Lisa M. Kaminskas, PhD^{a,d,**}

^aDrug Delivery Disposition and Dynamics, Monash Institute of Pharmaceutical Sciences, Parkville, VIC, Australia

^bARC Centre of Excellence in Convergent Bio-Nano Science and Technology, Melbourne, VIC, Australia

^cBio21 Institute, University of Melbourne, Melbourne, VIC, Australia

^dSchool of Biomedical Sciences, University of Queensland, St Lucia, QLD, Australia

Revised 5 August 2020

Abstract

Poly(lactide-co-glycolide) (PLGA) nanoparticles are one of the most commonly explored biodegradable polymeric drug carriers for inhaled delivery. Despite their advantages as inhalable nanomedicine scaffolds, we still lack a complete understanding of the kinetics and major pathways by which these materials are cleared from the lungs. This information is important to evaluate their safety over prolonged use and enable successful clinical translation. This study aimed to determine how the size and charge of ³H-labeled PLGA nanoparticles affect the kinetics and mechanisms by which they are cleared from the lungs and their safety in the lungs. The results showed that lung clearance kinetics and retention patterns were more significantly defined by particle size, whereas lung clearance pathways were largely influenced by particle charge. Each of the nanoparticles caused transient inflammatory changes in the lungs after a single dose that reflected lung retention times.

© 2020 Elsevier Inc. All rights reserved.

Key words: PLGA; Nanoparticles; Lungs; Clearance; Pharmacokinetics

While nanomaterials based on lipids (eg, liposomes and solid lipid nanoparticles) are most commonly explored as inhalable drug delivery systems,^{1,2} several polymeric nanomaterials (such as dendrimers and those based on chitosan or poly(lactide-co-glycolide); PLGA) have also attracted significant interest for this purpose.³⁻⁶ The pulmonary delivered drug-loaded polymeric and lipid based nanomaterials can significantly improve therapeutic efficacy against lung diseases (such as cystic fibrosis, lung cancer, asthma and pulmonary hypertension) and limit systemic side effects compared to the inhaled or oral delivery of small molecule drugs.¹⁻⁴ This is due to the ability of these nanomaterials to allow the slow and prolonged release of drug in

the lungs directly at the site of action, coupled with reduced drug concentrations in the blood.

Among the polymeric systems, PLGA nanoparticles are the most widely explored drug carriers for inhalable nanomedicines.^{1,3,7} They are highly biocompatible and can be customized to exhibit defined surface and other physicochemical properties and in vivo biodegradation rates. These desirable and tuneable properties make them potentially more suitable as drug delivery systems than lipid nanoparticles.^{7,8} Additionally, PLGA nanoparticles exhibit good nebulization stability.^{1,7,8} Despite the advantages of PLGA as a scaffold for inhalable nanomedicines, there is still a significant gap in our understanding of the kinetics and major pathways by which these polymeric nanomaterials (unlike loaded drugs) are cleared after pulmonary administration. This information is critical to evaluating their safety over prolonged use and in enabling their successful clinical translation as inhalable nanomedicines (Arikayce, report no: EMA/493973/2016). For example, to date, the lung clearance of pulmonary dosed PLGA nanoparticles has been assessed by bulk-labelling with technetium, or via tracking the pharmacokinetics of loaded drug, with no subsequent evaluation of the radiolabeled

*Correspondence to: M. Whittaker, ARC Centre of Excellence in Convergent Bio-Nano Science and Technology, Monash Institute of Pharmaceutical Sciences, Parkville, VIC, Australia, 3052.

**Correspondence to: L.M. Kaminskas, School of Biomedical Sciences, University of Queensland, St Lucia, QLD, Australia, 4072.

E-mail addresses: michael.whittaker@monash.edu, (M. Whittaker), l.kaminskas@uq.edu.au. (L.M. Kaminskas).

t1.1 Table 1
 t1.2 Physicochemical characterization of the ³H- and rhodamine-labeled PLGA nanoparticles via dynamic light scattering (represented as mean ± SD of 3 runs).

t1.3 Nanoparticles	Mean particle size (nm) ± S.D.	Mean PDI ± S.D.	Mean zeta potential (mV) ± S.D.
t1.4 ³ H-PLGA PF68 nanoparticles (~150 nm)	176 ± 2	0.09 ± 0.03	-26 ± 0
t1.5 ³ H-PLGA PVA nanoparticles (~150 nm)	173 ± 4	0.16 ± 0.01	-1 ± 0
t1.6 ³ H-PLGA CS nanoparticles (~150 nm)	202 ± 3	0.15 ± 0.01	+31 ± 3
t1.7 ³ H-PLGA PF68 nanoparticles (~50 nm)	60 ± 1	0.10 ± 0.01	-29 ± 0
t1.8 ³ H-PLGA PF68 nanoparticles (~400 nm)	485 ± 10	0.37 ± 0.03	-20 ± 0
t1.9 Rhodamine-PLGA PF68 nanoparticles (~150 nm)	159 ± 3	0.12 ± 0.01	-15 ± 1
t1.10 Rhodamine-PLGA PVA nanoparticles (~150 nm)	186 ± 2	0.09 ± 0.03	-1 ± 0
t1.11 Rhodamine-PLGA CS nanoparticles (~150 nm)	138 ± 1	0.20 ± 0.02	+38 ± 2
t1.12 Rhodamine-PLGA PF68 nanoparticles (~50 nm)	60 ± 1	0.13 ± 0.02	-11 ± 0
t1.13 Rhodamine-PLGA PF68 nanoparticles (~400 nm)	266 ± 4	0.52 ± 0.05	-5 ± 0

57 species being measured. These approaches typically poorly reflect
 58 the true kinetics of the polymer and nanoparticle.³ Further, the
 59 immunological response of the lungs to inhalable nanomedicines
 60 typically depends on the physicochemical properties and lung
 61 residence time of the inhaled nanoparticles, rather than the drug
 62 alone,^{3,9,10} together with 'particle load' in the lungs.^{11,12} In
 63 particular, particle size and surface charge affect the way in which
 64 nanoparticles interact with cellular and non-cellular barriers found
 65 within the lungs which are fundamentally important in driving
 66 pharmacokinetics and inflammatory effects.^{13–17} This highlights the
 67 importance of better understanding how the physicochemical
 68 properties of PLGA nanoparticles affect their lung clearance kinetics
 69 and pathways, and how this ultimately dictates the immunological
 70 response of the lungs.

71 This study initially aimed to characterize the intravenous and
 72 pulmonary pharmacokinetics and lung clearance of an anionic
 73 150 nm PLGA nanoparticle in rats by following tritium labeled
 74 (³H-lactide) PLGA. Since PLGA nanoparticles of varying size
 75 and charge have been evaluated as drug carriers in pre-clinical
 76 studies, the effect of these properties on patterns of lung retention
 77 and clearance were then evaluated. These goals were achieved by
 78 synthesizing PLGA nanoparticles of 50, 150 or 400 nm, with
 79 zeta potentials ranging from -30 and +30 mV. The impact that
 80 nanoparticle physicochemical properties and/or lung clearance
 81 kinetics have on the inflammatory response of the lungs to a
 82 single pulmonary dose was then evaluated by examining changes
 83 in cell numbers, levels of total protein and key cytokine markers
 84 of lung inflammation over 7 days.

85 Methods

86 Material

87 A detailed list of reagents used and the protocols described
 88 here are given in detail in the supporting information.

89 Animals

90 Monash Animal Services (VIC, Australia) supplied the
 91 Sprague–Dawley rats (male, 7–9 weeks). All animal experiments
 92 carried out in this manuscript were approved by the Monash
 93 Institute of Pharmaceutical Sciences Animal Ethics Committee.
 94 Rats used in this study were housed in microisolators with
 95 temperature-controlled environment (21–22 °C) and free access
 96 to water, on a 12 h light/dark cycle. Rats were provided unlimited

access to food with the exception of fasting post-surgery and up 97
 to 8 h post dosing. 98

99 Synthesis and characterization of ³H-labeled PLGA nanopar- 100 ticles

101 Linear ³H-PLGA was initially synthesized from custom 101
 purchased ³H-lactide. This, or commercially available 102
 rhodamine-PLGA were then used to synthesize the PLGA 103
 nanoparticles of various size and surface charge as described 104
 previously¹⁸ and in the supporting information. Table 1 105
 summarizes the nanoparticles prepared and their physicochemical 106
 properties. 107

108 Pharmacokinetics and lung clearance of ³H-PLGA nanoparticles

109 The plasma pharmacokinetics, excretion and organ biodis-
 tribution of the 150 nm anionic ³H-PLGA nanoparticle was 110
 initially evaluated in 3 groups of rats over 7 days: a) pulmonary 111
 dosed (intratracheal liquid instillation) – group 1 b) IV dosed – 112
 group 2 c) orally dosed – group 3. Rats in groups^{1–3} were 113
 surgically implanted with a cannula in the right carotid artery as 114
 previously described to facilitate serial blood sampling.^{19,20} 115
 Rats in group 2 were also cannulated via the right jugular vein to 116
 allow IV dosing. Rats were monitored overnight post-surgical 117
 implantation of cannula. The following day, rats were dosed with 118
³H-PLGA nanoparticles in sterile saline (150 µl for pulmonary 119
 dosing, 1 ml for IV and oral dosing) to provide a final dose of 5 120
 mg/kg ³H-PLGA and serial blood (200–250 µl), urine and feces 121
 sampled over 7 days as previously described.^{21,22} The ³H 122
 content of plasma, urine and feces was quantified via scintillation 123
 counting as previously described.^{22,23} Rats were euthanized 124
 after collection of the last blood sample via exsanguination under 125
 isoflurane and bronchoalveolar lavage fluid (BALF) and major 126
 organs collected as previously described.^{22,23} 127

128 A separate cohort of rats were then dosed with each of the ³H-
 PLGA nanoparticles in Table 1 via the lungs (n = 9 rats per 129
 nanoparticle). Three rats were sacrificed for each nanoparticle at 130
 1, 3 or 7 days after dosing and separate BALF and lung tissue 131
 collected to evaluate the lung clearance rate of the PLGA 132
 nanoparticles and quantify alveolar cells and levels of inflam- 133
 matory cytokines in the BALF over time. BALF samples were 134
 initially centrifuged to separately collect cells before BALF 135
 supernatant was quantified for ³H. Biodistribution in major 136
 organs was evaluated as previously described after 7 days 137
 only.²⁴ 138

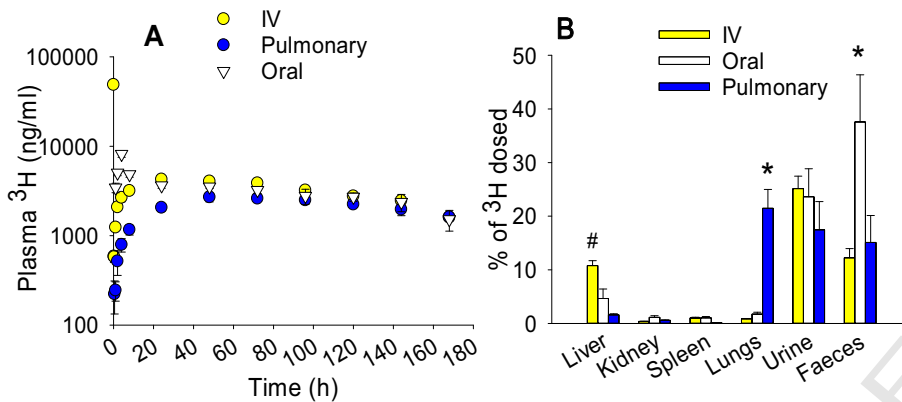


Figure 1. (A) Plasma concentration-time profiles of ~150 nm anionic ^3H -PLGA nanoparticles after IV, pulmonary and oral dosing to rats and (B) biodistribution of the ^3H -dose in major organs and total excreta after 7 days. Plasma concentrations are normalized to a dose of 5 mg/kg. Data represent mean \pm SD (n = 3–4 rats). *represents $p < 0.05$ cf. all other groups. # represents $p < 0.05$ cf pulmonary.

139 Speciation of ^3H in biological samples

140 We identified the molecular nature of ^3H species, as either
 141 intact nanoparticle, PLGA fragment, liberated ^3H -lactide or
 142 protein-bound ^3H -lactide/polymer fragment respectively in the
 143 BALF, lung tissue homogenate supernatant, urine and plasma,
 144 using size exclusion chromatography (SEC) on a superose
 145 column as previously described.^{22,23}

146 Lung deposition and alveolar macrophages uptake of 147 rhodamine-labeled PLGA nanoparticles

148 To determine the distribution pattern of PLGA nanoparticles in
 149 the lungs and their alveolar macrophages uptake, rats were dosed
 150 with PLGA nanoparticles labeled with rhodamine via the lungs as
 151 described earlier. Rats were sacrificed at two time points i.e.
 152 immediately, or 3 days after pulmonary dosing and the excised
 153 lungs were imaged via a Caliper IVIS Lumina II in vivo imager as
 154 reported earlier.²² A separate group of rats (n = 1 per nanoparticle)
 155 were sacrificed 24 h after lung administration of rhodamine-
 156 labeled nanoparticle. BALF was then collected and a 200–250 μl
 157 aliquot added onto a 35 mm μ -Dish (Ibidi GmbH, Germany),
 158 treated with DAPI nuclear stain (1:100 dilution) and cells analyzed
 159 by a fluorescence microscope (Leica TCS SP8, Germany).²⁵

160 Measurements of alveolar cell counts, total protein and 161 inflammatory cytokines in BALF

162 The inflammatory effect of PLGA nanoparticles on the lungs
 163 was determined via the differential quantification of alveolar
 164 macrophages, neutrophils and T-lymphocytes in the BALF cell
 165 fraction via flow cytometry, and by quantifying the levels of total
 166 protein and inflammatory cytokines (TNF- α , IL-1 β and MCP-1) in
 167 the BALF supernatant via ELISA as previously described.²⁵
 168 Negative control rats were dosed with saline via the lungs and
 169 euthanized 7 days later, while positive control rats were dosed with
 170 LPS or NiO and euthanized after 4 h and 7 days respectively.

171 Non-compartmental pharmacokinetic analysis and statistics

172 The plasma levels of ^3H derived from the PLGA nanoparticles
 173 was measured by converting nanoparticle radioactivity (in $\mu\text{Ci}/\text{mg}$)

Table 2

Apparent plasma pharmacokinetic parameters of ~150 nm anionic ^3H -PLGA nanoparticles after pulmonary, IV and oral dosing in rats (5 mg/kg). Data are represented as mean \pm SD, n = 3–4. *represents $p < 0.05$ cf. IV. # represents $p < 0.05$ cf oral.

	IV	Pulmonary	Oral	
K_{el} (h^{-1})	0.007 \pm 0.000	0.005 \pm 0.000*	0.006 \pm 0.002	t2.1
$T_{1/2}$ (h)	94.6 \pm 5.2	138 \pm 9*	117 \pm 31	t2.2
$AUC_{0-\infty}$ ($\mu\text{g}/\text{ml}\cdot\text{h}$)	765 \pm 47	688 \pm 58	800 \pm 178	t2.3
AUC_{0-7} ($\mu\text{g}/\text{ml}\cdot\text{h}$)	546 \pm 20	359 \pm 17*#	526 \pm 42	t2.4
V_c (ml)	32 \pm 3	-	-	t2.5
T_{max} (h)	-	60 \pm 14#	4 \pm 0	t2.6
C_{max} ($\mu\text{g}/\text{ml}$)	-	2.7 \pm 0.3#	8.2 \pm 0.6	t2.7
$F_{abs}^{0-\infty}$ (%)	-	90 \pm 7	104 \pm 23	t2.8
F_{abs}^{0-7} (%)	-	48 \pm 2#	69 \pm 5	t2.9
% dose in urine	25 \pm 2	18 \pm 5	24 \pm 5	t2.10
% dose in feces	12 \pm 2	15 \pm 5#	38 \pm 9	t2.11

to ng/ml. Plasma concentrations and pharmacokinetic parameters of ^3H -PLGA nanoparticles however, were calculated on the assumption that ^3H remains associated with the intact nanomaterial. Since this is not the case, only ‘apparent’ pharmacokinetic parameters could be determined (as previously described^{21,22} and detailed in the supporting information). Statistical differences in BALF cell count between groups were calculated via one way ANOVA with Tukey’s test for least significant differences. Significance was determined at a level of $P < 0.05$.

183 Results

184 Plasma pharmacokinetics and biodistribution of 150 nm anionic 185 ^3H -PLGA nanoparticles after intravenous, pulmonary and oral 186 administration to rats

187 Plasma concentrations of ^3H were initially high after IV
 188 administration of 150 nm anionic PLGA (Figure 1, A, Table 2)
 189 owing to the presence of mainly intact ^3H -nanoparticle (Figure 2).
 190 However, plasma ^3H quickly decreased by 100-fold within 190
 191 10 min r, presumably as a result of rapid uptake by the liver and
 192 spleen. After 7 days though, only 11% of the dose was collectively

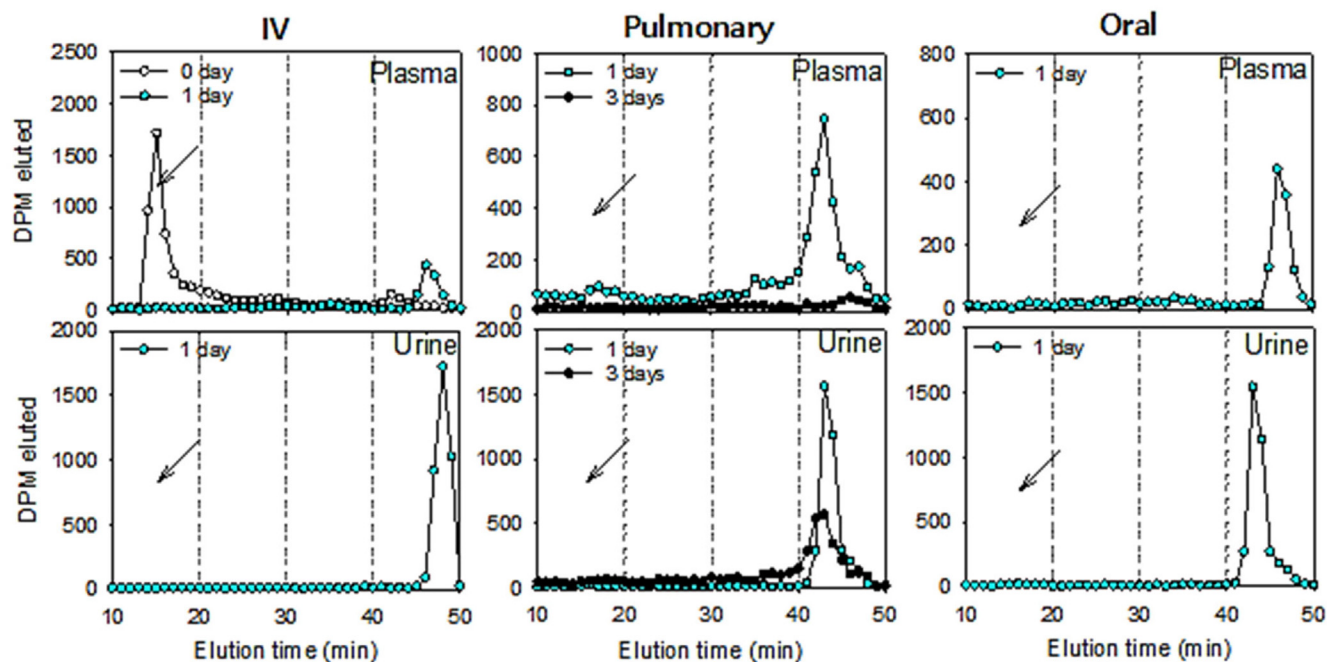


Figure 2. Size exclusion chromatography profiles of ^3H in plasma and urine collected 0, 1 or 3 days after IV, pulmonary and oral dosing of ~ 150 nm anionic ^3H -PLGA nanoparticles. Arrows specify the retention time of intact ^3H PLGA nanoparticles.

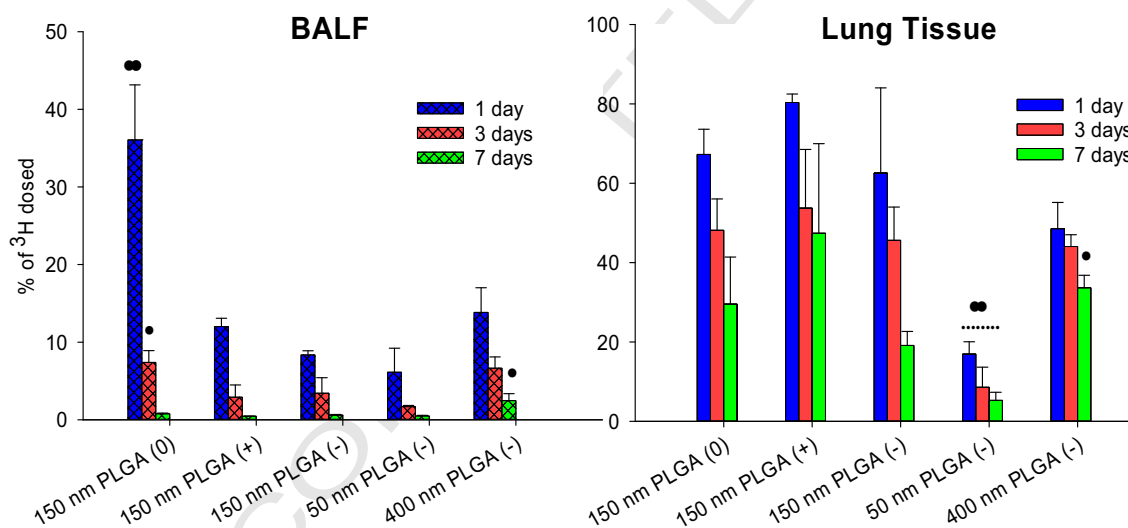


Figure 3. Proportion of ^3H -PLGA recovered in BALF and lung tissue over 7 days after pulmonary administration. Data are mean \pm SD ($n = 3-4$). * $P < 0.05$ compared to all other nanoparticles. # $P < 0.05$ compared to 50 and 150 nm PLGA (-). ^ $P < 0.05$ compared to 150 nm PLGA (+) and (-).

recovered in the liver and spleen, and little ^3H was recovered in the other organs (Figure 1, B). After 10 mins, a much slower plasma elimination phase was observed with an apparent terminal half-life of 4 days. The ^3H species present in plasma over this period however, was largely a low molecular weight product of PLGA hydrolysis that co-eluted with ^3H -lactide (see Figure 2, and Figure S5 in the supporting information) and was the primary ^3H product eliminated in urine (approx. 25% over 7 days). Elimination pharmacokinetics of the intact PLGA nanoparticle could therefore not be determined due to rapid polymer hydrolysis in vivo. It should be noted however, that a large proportion of intact PLGA nanoparticle was retained at the top

of the superose column, and as such, the true proportion of intact versus hydrolyzed products PLGA nanoparticles in plasma samples could not be quantified.

After pulmonary administration, ^3H species was slowly absorbed from the lungs and reached peak plasma concentrations after 2–3 days (Figure 1, A, Table 2). Thereafter, plasma ^3H concentrations persisted for a prolonged period of time, with an apparent half-life of 6 days. Again though, ^3H in plasma was mainly associated with low molecular weight products of PLGA hydrolysis (Figure 2). Apparent pulmonary bioavailability extrapolated to infinity ($F_{\text{abs}}^{0-\infty}$) was approx. 90%, suggesting efficient systemic access of ^3H -label. This was supported by the similar

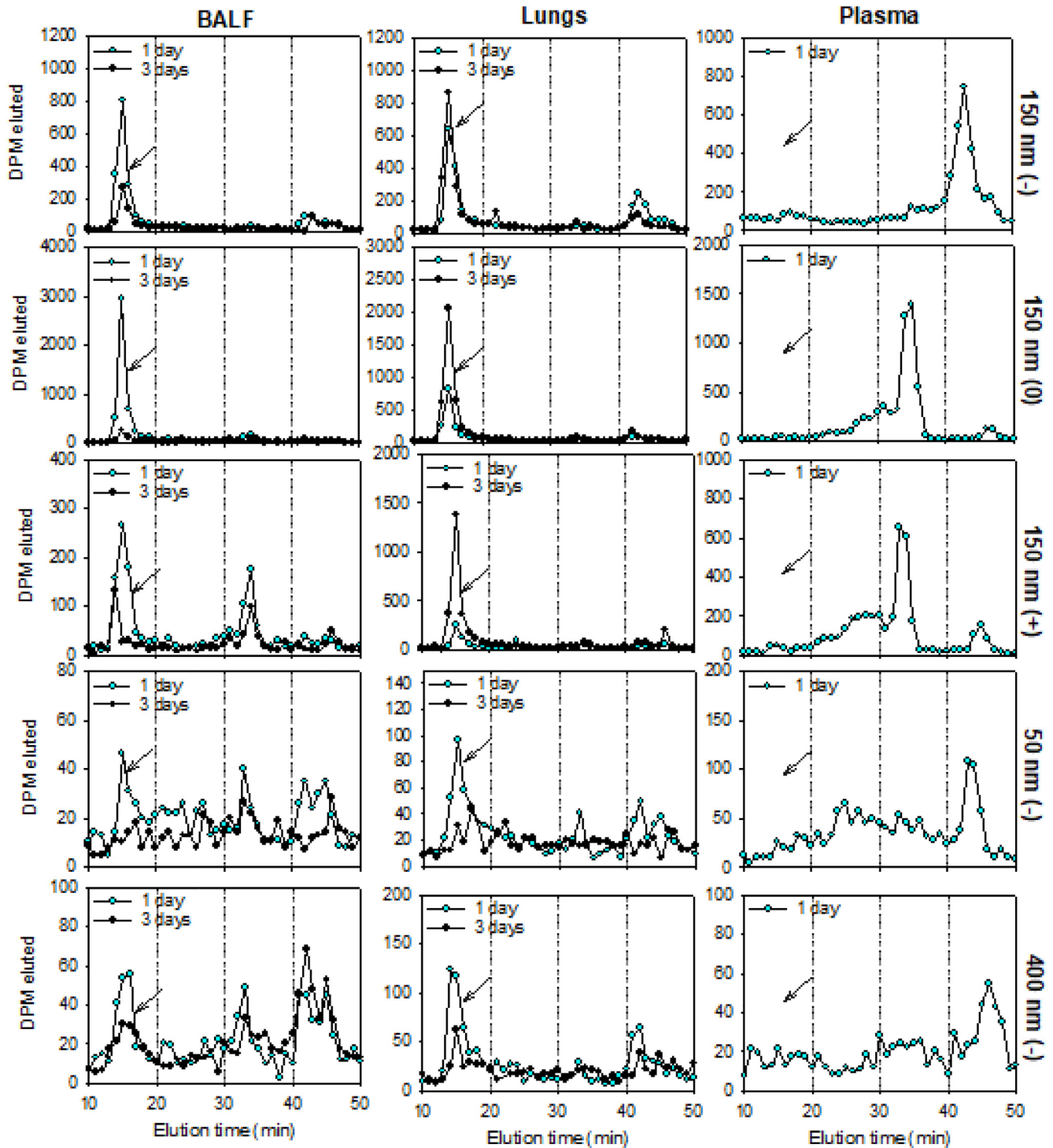


Figure 4. Size exclusion chromatography profiles of ^3H -PLGA nanoparticles in BALF, lung tissue homogenate supernatant and plasma after pulmonary administration to rats. Plasma profiles are only shown for day 1. Arrows specify the retention time of intact ^3H -PLGA nanoparticles.

217 recovery of the ^3H dose in urine and feces between pulmonary and
 218 IV dosed rats. Liver biodistribution after pulmonary administration
 219 was lower after 7 days compared to after IV administration, but this
 220 was likely due to the rapid removal of the IV dose by the liver,
 221 followed by gradual hydrolysis (Figure 1, B).

222 After oral administration however, apparent bioavailability
 223 extrapolated to infinity was approx. 100% and the fraction of the

dose in urine was essentially identical to that after IV 224
 administration (Figure 1, A, Table 2). While recovery of the 225
 dose in feces appeared to be two-fold higher than after IV 226
 administration, the data suggested that the ^3H -lactide, when 227
 incorporated into PLGA polymers and nanoparticles, is essentially 228
 completely absorbed from the gastrointestinal tract of rats 229
 after oral administration. As a result, it is not possible to evaluate 230

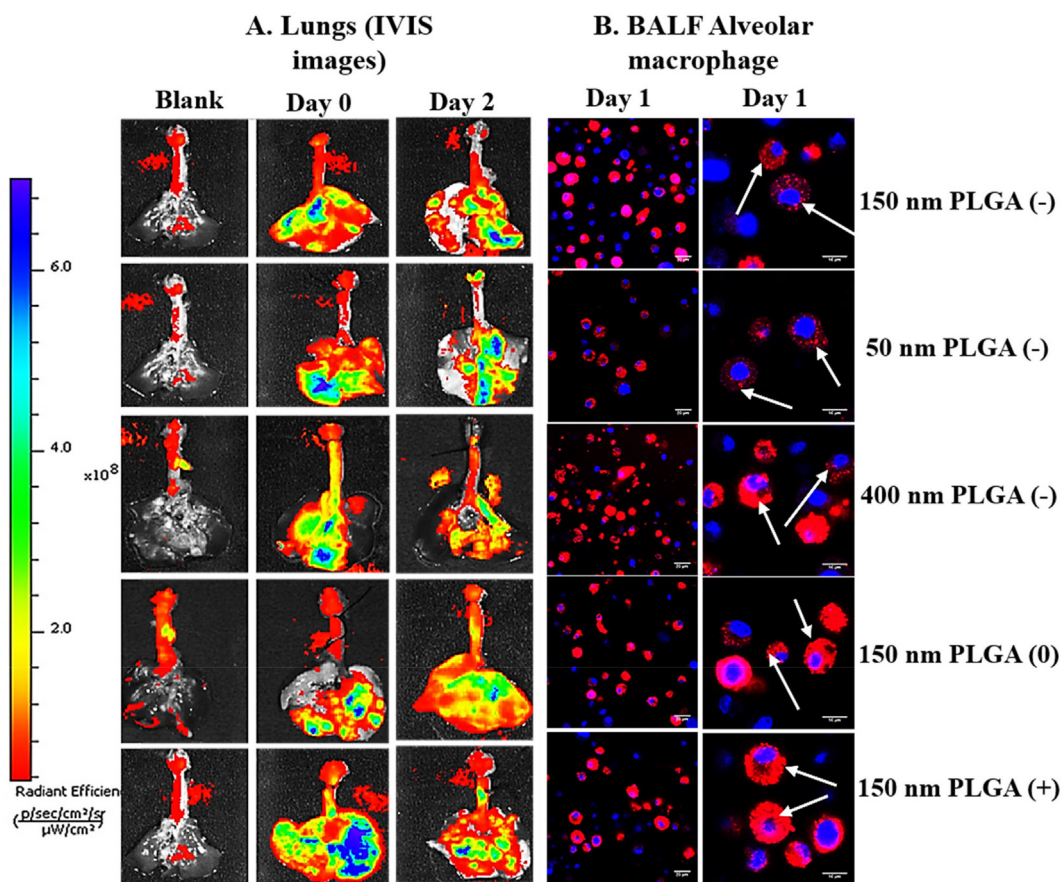


Figure 5. (A) Lung deposition of rhodamine-labeled PLGA nanoparticles immediately and 2 days after pulmonary administration to rats. Blank represents background lung fluorescence. (B) Uptake of PLGA nanoparticles by alveolar macrophages of rats 24 h post pulmonary administration. The individual nanoparticles located within macrophages are shown by arrows. Red - rhodamine-labeled PLGA nanoparticles; blue - DAPI stained nuclei. Microscope images (B) were acquired using a 60x objective at zoom factor 1.0 (scale bar 20 μ m) and 1.5 (scale bar 10 μ m).

231 the exact fraction of a pulmonary dose of PLGA nanoparticle
 232 removed from the lungs by the mucociliary clearance, since the
 233 nanoparticles (or at least the lactide content of the nanoparticle)
 234 are rapidly biodegraded in vivo and completely absorbed from
 235 the gut.

236 Pulmonary retention and speciation of 3 H-labeled PLGA 237 nanoparticles in the lungs and plasma

238 To more widely evaluate the lung clearance rate of 3 H-PLGA
 239 nanoparticles of different size and charge, the proportion of
 240 intratracheal administered 3 H-label remaining in the BALF and
 241 lung tissue over 7 days after pulmonary dosing in rats was
 242 quantified (Figure 3 and supporting information). After pulmo-
 243 nary dosing, distinct differences in the lung distribution and
 244 clearance rate of each of the PLGA nanoparticles were observed.
 245 Interestingly, the ~150 nm uncharged and cationic PLGA
 246 nanoparticles exhibited little to no lung clearance over the first
 247 24 h after pulmonary dosing. In contrast, approximately 80% of
 248 the ~50 nm anionic nanoparticles were cleared from the lungs in
 249 this time. With the exception of the uncharged ~150 nm PLGA
 250 nanoparticles, where approximately 30% of the remaining dose
 251 was recovered in the BALF after 1 day, 3 H-label from the other
 252 PLGA nanoparticles were mainly associated with lung tissue. In

general, the PLGA nanoparticles were initially cleared from the 253
 lungs in the order ~150 nm uncharged = ~150 nm cationic >150 254
 nm anionic = ~400 nm anionic >50 nm anionic. Thereafter, the 255
 ~400 nm anionic nanoparticles exhibited the slowest rate of lung 256
 clearance over 1 week, while unsurprisingly, the ~50 nm 257
 nanoparticles were most rapidly cleared. Little difference was 258
 observed in the effect of nanoparticle charge on lung retention 259
 after 7 days, although the cationic nanoparticle exhibited a 260
 slightly, but not statistically different, greater retention in the 261
 lungs after 1 week (see supporting information). 262

The SEC profiles indicated that the primary 3 H species 263
 present in the BALF and lung tissues over 3 days largely 264
 corresponded to intact PLGA nanoparticles (Figure 4). Tritium 265
 levels beyond 3 days could not be quantified. There was 266
 significant evidence though, of extensive polymer and nanopar- 267
 ticle erosion and hydrolysis (as peptide fragments or free lactide) 268
 in the plasma and BALF, particularly for the 50 and 400 nm 269
 nanoparticles. 270

Patterns of lung deposition after pulmonary administration 271

The deposition pattern of rhodamine-labeled PLGA nanoparticles 272
 were examined by the IVIS images of the excised lungs immediately, 273
 and 2 days after pulmonary administration (Figure 5, A). The results 274

275 show that the PLGA nanoparticles, irrespective of their size and
 276 charge, were deposited equally in the upper and lower respiratory
 277 regions immediately after dosing, with most generally localized to
 278 deeper regions of the lungs within 2 days. The 400 nm anionic
 279 nanoparticle however, appeared to be localized mainly in the central
 280 region of the lungs after 2 days (showing inhomogeneous distribution
 281 and potential localization in the larger airways), while the 50 nm
 282 anionic nanoparticles showed evidence of more accelerated lung
 283 clearance compared to the other nanoparticles. There were little
 284 apparent differences between the lung distribution of the 150 nm
 285 nanoparticles with different charges.

286 Confocal images of alveolar macrophages obtained from
 287 BALF after 24 h (Figure 5, B) revealed that the nanoparticles
 288 were present in large vacuoles within these cells. Although a
 289 diffuse fluorescent labelling was also present throughout the
 290 cytosol, but this was likely due to the liberated rhodamine.^{26,27}
 291 In general though, the anionic ~150 nm and 50 nm nanoparticles
 292 showed the lowest uptake by macrophages, consistent with lung
 293 clearance rates (Figure 3).

294 Organ biodistribution 7 days after pulmonary administration

295 Seven days after pulmonary administration of the ³H-labeled
 296 PLGA nanoparticles, the dose showed limited uptake in the liver
 297 ($\leq 2\%$), kidneys ($< 0.6\%$) and spleen ($< 0.3\%$), with the exception
 298 of anionic ~50 nm particles where the fraction of the ³H-dose
 299 recovered in these organs was moderately (though not
 300 significantly) higher, at approximately 4%, 1.4% and 0.6%
 301 respectively (Figure 6). The proportion of the ³H-dose recovered
 302 in feces was generally 10–15%, but was significantly lower for
 303 the ~150 nm cationic nanoparticles (approx. 3%). The proportion
 304 of ³H-dose excreted in urine was 17–20% for all nanoparticles
 305 with the exception of the ~50 nm nanoparticles where more than
 306 30% of the ³H-dose was recovered in urine, likely as ³H-lactide.

307 Pro-inflammatory effects of PLGA nanoparticles in the lungs

308 The pro-inflammatory effects of the PLGA nanoparticles post
 309 single 5 mg/kg pulmonary dose in rats was examined by
 310 comparing changes in total and differential alveolar macrophage,
 311 neutrophil and T-lymphocyte cell counts and cytokine, protein
 312 and LDH levels in the BALF to the rats dosed with LPS or NiO
 313 nanoparticles (positive controls) and saline (negative control)
 314 (Figure 7). Total cell numbers in the BALF of PLGA
 315 nanoparticles dosed rats, irrespective of size and charge, were
 316 significantly elevated when compared to the negative control
 317 group. With the exception of the 400 nm PLGA nanoparticles
 318 that show prolonged lung retention however, total cell numbers
 319 declined over the next 7 days for all nanoparticles. Alveolar
 320 macrophages were initially elevated slightly for anionic and
 321 uncharged ~150 nm PLGA nanoparticles and anionic ~400 nm
 322 nanoparticles when compared to saline dosed rats. Neutrophil
 323 counts were significantly higher at all times with the exception of
 324 anionic ~150 nm and ~50 nm nanoparticles, where neutrophil
 325 counts declined to similar levels to saline dosed rats within 7
 326 days post dose. T lymphocyte counts were raised for the anionic
 327 ~400 nm nanoparticles over 7 days and 1 day after dosing for the
 328 ~150 and ~50 nm anionic nanoparticles.

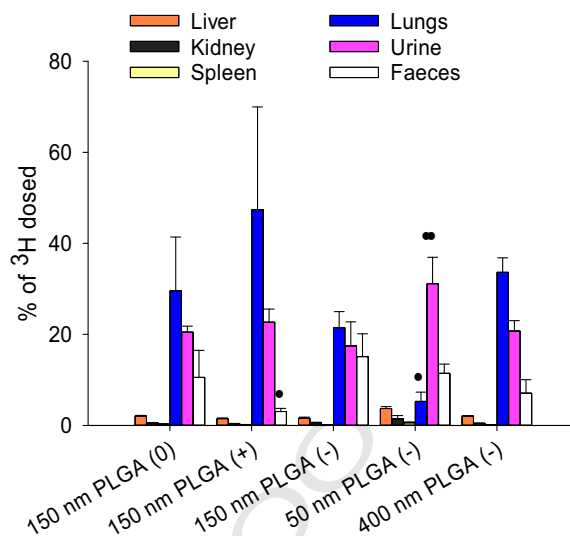


Figure 6. Biodistribution of ³H-PLGA nanoparticles following pulmonary administration to rats. *Represents $p < 0.05$ cf. equivalent parameter for all other group. Values represent mean \pm SD (n = 3–4 rats).

TNF α and MCP-1 levels were found elevated in the BALF of 329 almost all rats over 7 days given PLGA nanoparticles 330 irrespective of surface charge or particle size (Figure 7). In 331 general, no significant elevations in IL-1B concentrations were 332 observed over 7 days with the exception of the cationic 333 nanoparticles after 3 days. Total protein concentration in the 334 BALF was unchanged after PLGA administration, but was 335 elevated in the positive controls (Figure 7). 336

337 Discussion

The present study showed that ³H-labeled PLGA nanopar- 338 ticles do not appear to be absorbed intact from the lungs after 339 pulmonary administration, but rather, are degraded into lower 340 molecular weight peptide/oligomer and amino acid constituents 341 that are subsequently absorbed. This is consistent with previous 342 reports which suggest limited absorption of intact biodegradable 343 nanomaterials from the lungs.^{22,23,28–30} At the same time 344 though, intact PLGA nanoparticles were rapidly cleared from the 345 plasma after IV dosing, although it is unclear from this study 346 whether this occurred as a result of uptake by the liver or spleen 347 or hydrolysis in plasma. *Importantly though, the absolute 348 proportion of the ³H dose (as amino acid or oligomer, etc.) 349 removed from the lungs by the mucociliary escalator could not 350 be accurately quantified due to extensive absorption of liberated 351 lactide from the gastrointestinal tract. This appeared, however, 352 to be limited when compared to lipid-based nanoparticles.*²² 353 This is in contrast to the results of other research groups which 354 generally attribute mucociliary removal as the primary lung 355 clearance pathway for macromolecules (e.g. proteins, dendrimers) 356 and both biodegradable and non-biodegradable 357 nanoparticles.^{21,22} 358

Despite the limitations in accurately quantifying the mucociliary 359 clearance of PLGA nanoparticles, this was found to be significantly 360 affected by changes in the physicochemical properties (i.e. surface 361

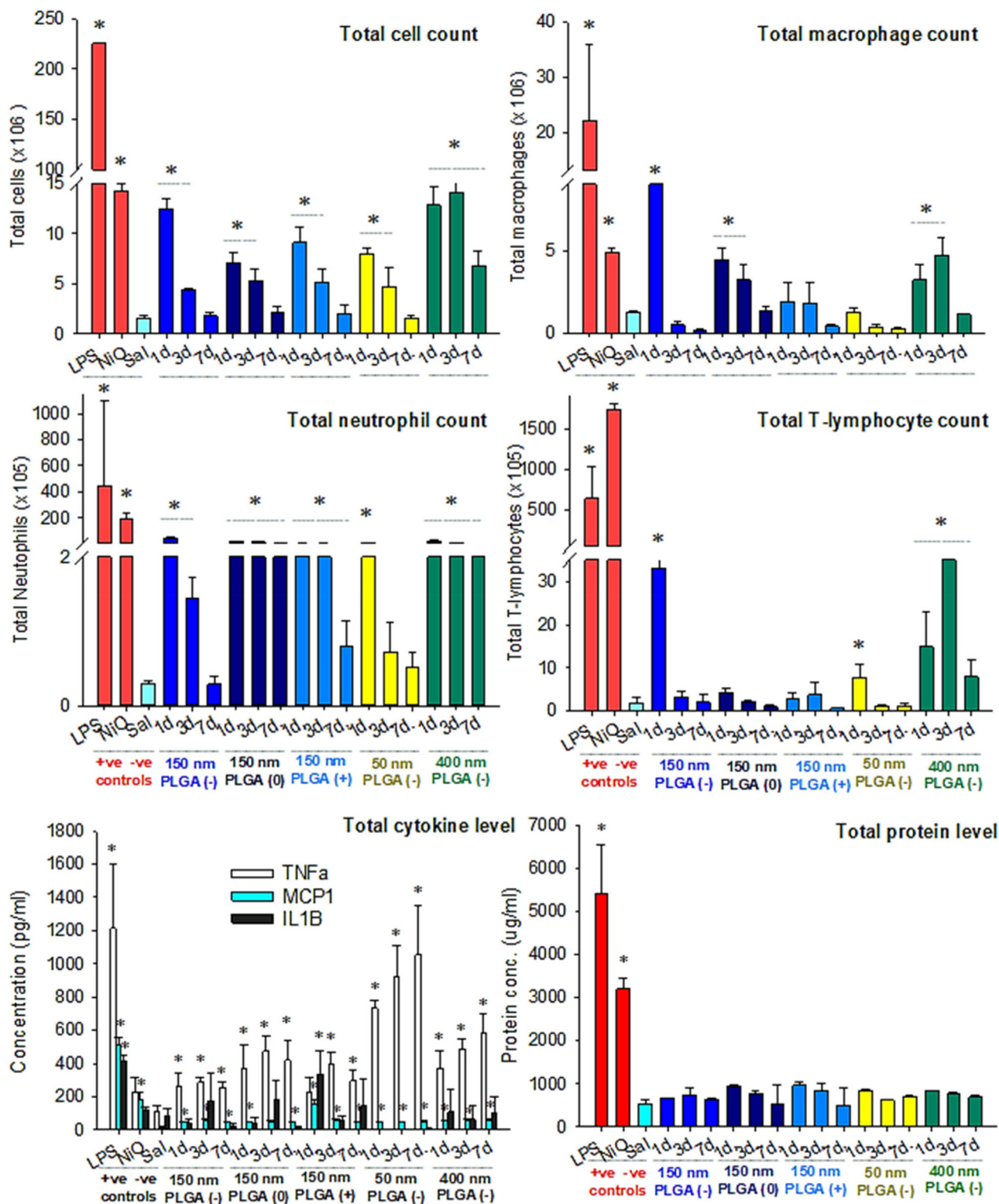


Figure 7. Differential cell counts, cytokine concentrations and total protein level in the BALF of rats dosed with saline (Sal), lipopolysaccharide (LPS), NiO nanoparticles, and PLGA nanoparticles over 7 days. Data represent mean \pm SD (n = 3–4 rats). *P < 0.05 compared to saline.

charge and size) as shown earlier for other nanomaterials.³¹ The present study shows that for identical sized PLGA nanoparticles, positive charge significantly reduces mucociliary clearance when

compared to uncharged or anionic nanoparticles (consistent with the results of others), as a result of increased retention of the cationic particles in the lungs through electrostatic interactions with epithelial

368 and mucus membranes.^{13,32} For example, these finding are similar
369 to those of a previous study where mucociliary clearance of cationic
370 PLGA-CS (163 nm) nanoparticles was reported to be 4–5 times
371 lower than the negatively charged PLGA (157 nm) or PEG-PLGA
372 (389 nm) nanoparticles in a trachea based in vitro model.¹³
373 Mucociliary clearance was unaffected though, by changes in
374 nanoparticle size, despite differences in lung clearance rates.

375 Mucociliary clearance is highly dependent on the site of
376 nanoparticle deposition within the lungs.^{3,13,22,33} Upon deposi-
377 tion in the tracheobronchial region, nanoparticles undergo an initial
378 rapid clearance phase via the mucociliary escalator. However,
379 transport within or possibly across the mucus layer can be low due
380 to adhesive interactions between particles with hydrophobic or
381 hydrophilic regions of mucins, leading to subsequent changes in
382 overall mucus transport properties.^{3,13,22,33} In contrast, peripheral
383 and alveolar clearance of particles by macrophages is a much
384 slower process which lasts from days to weeks.^{3,13,22,33} In the
385 present study the lung deposition studies clearly showed that
386 PLGA nanoparticles were localized in the deeper region of the
387 lungs within 2 days after dosing. From here, overall clearance is
388 based on alveolar macrophage uptake, rate of biodegradation and
389 absorption, and interactions with the lung epithelium in addition to
390 mucociliary elimination.^{3,4,33} For this reason, mucociliary
391 elimination is only one of many factors that contribute to overall
392 lung clearance for PLGA nanoparticles that are deposited in the
393 deeper lungs. Further, multiple studies have shown that mucociliary
394 clearance of particles with sizes less than 6 μm do not differ
395 significantly, due to the size limit of the irregular mesh-like
396 network of mucus.^{34,35} Therefore, particle size of PLGA
397 nanoparticles (50–400 nm) in the current study was not found to
398 have a significant impact on the mucociliary clearance.

399 The particle size of PLGA nanoparticles was, however, found to
400 have a major impact on their lung retention patterns as well as rates of
401 lung clearance. Notably, within 1 day after pulmonary dosing, most
402 of the ³H label remaining in the lungs (identified mainly as intact
403 nanoparticle) was associated with the lung tissues, with only a small
404 proportion associated with the BALF. This suggests that PLGA
405 nanoparticles show highly efficient mucus penetrating capabilities,
406 allowing them to gain access to the absorptive epithelial surface of
407 the lungs. An increase in particle size was found to enhance long
408 term lung retention, although the 400 nm nanoparticles showed
409 initial (24 h) rapid clearance from the lungs which may have been
410 due to initial mucociliary elimination based on the tracheal location
411 of the dose immediately after intratracheal instillation. Likewise, the
412 ~50 nm anionic nanoparticle showed the most rapid lung clearance
413 and highest proportion of urinary elimination indicating its high
414 systemic absorption via lung epithelium. The results of the present
415 study indicate that pulmonary delivered PLGA nanoparticles
416 endured in vivo bioerosion within the lungs over 7 days that
417 contributed in large part to their elimination from the lungs. This was
418 reflected in the urinary elimination of the pulmonary ³H dose, where
419 the primary ³H species eliminated via the urine appeared to be
420 liberated lactide. Other work has similarly shown that the rate of
421 degradation of a smaller PLGA nanoparticle was faster than a larger
422 PLGA nanoparticle because the higher surface area to volume ratio
423 of the smaller particle.^{36,37} To the best of our knowledge, though, no
424 in vivo studies to date have examined the impact of inhaled PLGA
425 nanoparticle size on their lung disposition and retention. Despite the

biodegradable nature of PLGA nanoparticles, our results are also
426 consistent with those of non-biodegradable inorganic nanoparticles,
427 where lung clearance rates have been reported to be inversely
428 proportional to size, and extra-pulmonary translocation is directly
429 proportional to particle size.^{15,16,38}
430

431 In contrast to the effect of size, changes in nanoparticle charge
432 were found to have relatively minimal impacts on rates of lung
433 clearance and disposition of PLGA nanoparticles, although cationic
434 PLGA nanoparticles unsurprisingly exhibited the slowest rate of
435 lung clearance over 7 days. Uptake by alveolar macrophages also did
436 not appear to have a significant impact on lung clearance rates. One
437 of the likely explanations for these results is the interaction of PLGA
438 nanoparticles with biomolecules of the lung lining fluid, such as
439 phospholipids and proteins, leading to the formation of a protein/
440 lipid corona.^{39–41} It is well established that when exposed to
441 complex biological environment nanoparticles acquire a new
442 biological identity due to the rapid surface absorption of
443 biomolecules.^{39–41} Indeed studies have shown that surface
444 chemistry and charge of nanoparticles influence the initial adsorption
445 of lipids and proteins within lungs which can significantly change
446 the physiochemical properties of nanoparticles.^{39,41} For instance,
447 after incubation in the BALF of rats, the zeta potential of CeO₂ and
448 ZnO nanoparticles can undergo surface charge inversion from
449 positive to negative, with a corresponding increase in hydrodynamic
450 diameter and conductance.⁴¹ Although the composition of proteins
451 in the corona of these nanoparticles were similar (primarily
452 transferrin, albumin, α 1-antitrypsin), the amount of proteins detected
453 varied.⁴¹ To this point, however, it is difficult to establish the extent
454 to which the protein and lipid corona affects lung retention and
455 clearance of PLGA nanoparticles due to lack of sufficient studies in
456 this field.

457 Overall, lung retention data indicated that all PLGA nanopar-
458 ticles ≥ 150 nm displayed in general, sustained lung residence
459 (>20% dose retained in the lungs after 7 days). These results are
460 consistent with others who have reported the lung retention times
461 of PLGA nanoparticles in rodents using bulk-labelling approaches
462 (^{99m}Tc or ¹²⁵I-labeled) that do not give information about the
463 contribution of PLGA hydrolysis and nanoparticle erosion to lung
464 clearance.^{42–44} However, the total residence time of loaded drugs
465 (in PLGA nanoparticles) in BALF and lung tissues was
466 significantly shorter than the lung retention time of the PLGA
467 nanocarrier itself.^{45,46} This shows that the pulmonary clearance
468 kinetics of PLGA nanoparticle-loaded drugs differs significantly
469 when compared to the nanoparticle-based carriers.^{45,46} Neverthe-
470 less, it is evident from this study that more work is needed to fully
471 describe the pulmonary pharmacokinetics of PLGA nanoparticles
472 and to better understand the individual fate of the PLGA polymers
473 and the nanoparticle itself.

474 In addition, the pulmonary clearance kinetics of nanoparticles
475 should be examined with their inflammatory effects on the lungs,
476 since local inflammatory reactions (transient or prolonged) can
477 have a substantial effect on lung clearance mechanisms,
478 pathways and kinetics.^{3,9,25} Also, the repeated dosing of
479 nanoparticles will likely elevate the nanomaterial lung burden
480 over time that could prove to be a major challenge in the
481 development of inhalable nanomedicines for chronic respiratory
482 diseases.⁴⁷ In general, transient elevations in lung immune cell
483 numbers, TNF α and MCP were observed after pulmonary

484 administration of 5 mg/kg for all PLGA nanoparticles, which is
 485 in agreement with previous results that have reported the
 486 presence of a short-lived inflammatory reaction in the lungs
 487 following pulmonary administration of nanomaterials.^{48,49} With
 488 the exception of the 400 nm anionic nanoparticles that exhibited
 489 the slowest lung clearance beyond 1 day, increases in cell
 490 numbers resolved by 7 days after a single dose. TNF and MCP
 491 concentrations in BALF, however, remained elevated over 1
 492 week, particularly for the 50 nm nanoparticles. To this end,
 493 patterns of lung inflammation were broadly consistent with rates
 494 of lung clearance of the nanoparticles and macrophage uptake
 495 with evidence of more prolonged lung inflammation for
 496 nanoparticles that were cleared slowest from the lungs. The
 497 exception to this however, is the prolonged increased TNF α
 498 concentrations in the BALF or rats administered the 50 nm
 499 particles which exhibit the fastest lung clearance and limited
 500 macrophage uptake. An explanation for this is unclear at this
 501 time. While these results suggest that PLGA nanoparticles may
 502 be more pro-inflammatory in the lungs than other biodegradable
 503 nanosized drug delivery systems (such as dendrimers, solid lipid
 504 nanoparticles and liposomes,⁵⁰⁻⁵⁵ the doses delivered here were
 505 also up to 5 fold higher than those used previously and may also
 506 reflect a higher degree of 'nanomaterial burden'.

507 Overall, the results have highlighted the importance of
 508 physiochemical properties (i.e. particle size and charge) in
 509 differentially dictating the kinetics and mechanisms by which
 510 pulmonary administered PLGA nanoparticles are cleared from
 511 the lungs and rates of hydrolysis and erosion. The data showed
 512 that lung clearance pathways were more significantly influenced
 513 by nanoparticle charge, whereas lung clearance kinetics and
 514 retention patterns of ³H-labeled PLGA nanoparticles were more
 515 significantly defined by particle size. Transient but reversible
 516 inflammatory changes were observed in the lungs after a single 5
 517 mg/kg pulmonary dose, which warrants further detailed
 518 investigations. Notably, the impact of the chronic use of inhaled
 519 PLGA nanoparticles on the lungs, optimal dosing schedules and
 520 the maximal tolerated dose needs to be investigated, ideally in
 521 large animals that more closely reflect human pulmonary
 522 pharmacokinetics.⁵⁶ In conclusion, this study provides important
 523 insights on the lung clearance mechanisms, pathways and
 524 pharmacokinetics that will be beneficial in the design and
 525 evaluation of not only PLGA based inhalable nanomedicines
 526 based but other polymeric nanoparticle delivery systems.

527 Funding and acknowledgement

528 SH was supported by a VIDS postgraduate scholarship. LMK
 529 was supported by an NHMRC Career Development fellowship.
 530 This work was partly funded by ARC Discovery and NHMRC
 531 Project grant schemes.

532 Conflict of interest

533 The authors declare no conflict of interest.

Appendix A. Supplementary data

534

Supplementary data to this article can be found online at 535
<https://doi.org/10.1016/j.nano.2020.102291>. Q4

References

537

538

1. Sung JC, Pulliam BL, Edwards DA. Nanoparticles for drug delivery to 539
the lungs. *Trends Biotechnol* 2007;**25**(12):563-570. 540
2. Patton JS, Byron PR. Inhaling medicines: delivering drugs to the body 541
through the lungs. *Nat Rev Drug Discov* 2007;**6**(1):67-74. 542
3. Haque S, Whittaker MR, McIntosh MP, Pouton CW, Kaminskas LM. 543
Disposition and safety of inhaled biodegradable nanomedicines: 544
opportunities and challenges. *Nanomedicine* 2016;**12**(6):1703-1724. 545
4. Marasini N, Haque S, Kaminskas LM. Polymer-drug conjugates as 546
inhalable drug delivery systems: a review. *Curr Opin Colloid Interface* 547
Sci 2017;**31**:18-29. 548
5. Kaminskas LM, McLeod VM, Ryan GM, Kelly BD, Haynes JM, 549
Williamson M, et al. Pulmonary administration of a doxorubicin- 550
conjugated dendrimer enhances drug exposure to lung metastases and 551
improves cancer therapy. *J Control Release* 2014;**183**:18-26. 552
6. Al-Qadi S, Grenha A, Carrión-Recio D, Seijo B, Remuñán-López C. 553
Microencapsulated chitosan nanoparticles for pulmonary protein 554
delivery: in vivo evaluation of insulin-loaded formulations. *J Control* 555
Release 2012;**157**(3):383-390. 556
7. Beck-Broichsitter M, Merkel OM, Kissel T. Controlled pulmonary drug 557
and gene delivery using polymeric nano-carriers. *J Control Release* 558
2012;**161**(2):214-224. 559
8. Ulery BD, Nair LS, Laurencin CT. Biomedical applications of 560
biodegradable polymers. *J Polym Sci Part B Polym Phys* 2011;**49** 561
(12):832-864. 562
9. Geiser M, Kreyling WG. Deposition and biokinetics of inhaled 563
nanoparticles. *Part Fibre Toxicol* 2010;**7**(2):1-17. 564
10. Geiser M, Schürch S, Gehr P. Influence of surface chemistry and 565
topography of particles on their immersion into the lung's surface-lining 566
layer. *J Appl Physiol* 2003;**94**(5):1793-1801. 567
11. Oberdorster G. Lung particle overload: implications for occupational 568
exposures to particles. *Regul Toxicol Pharmacol* 1995;**21**(1):123-135. 569
12. Oberdörster G. Lung clearance of inhaled insoluble and soluble particles. 570
J Aerosol Med 1988;**1**(4):289-330. 571
13. Henning A, Schneider M, Nafee N, Muijs L, Rytting E, Wang X, et al. 572
Influence of particle size and material properties on mucociliary 573
clearance from the airways. *J Aerosol Med Pulm Drug Deliv* 2010;**23** 574
(4):233-241. 575
14. Schneider CS, Xu Q, Boylan NJ, Chisholm J, Tang BC, Schuster BS, 576
et al. Nanoparticles that do not adhere to mucus provide uniform and 577
long-lasting drug delivery to airways following inhalation. *Sci Adv* 578
2017;**3**(4)e1601556. 579
15. Nemmar A, Hoet PM, Vanquickenborne B, Dinsdale D, Thomeer M, 580
Hoylaerts M, et al. Passage of inhaled particles into the blood circulation 581
in humans. *Circulation* 2002;**105**(4):411-414. 582
16. Furuyama A, Kanno S, Kobayashi T, Hirano S. Extrapulmonary 583
translocation of intratracheally instilled fine and ultrafine particles via 584
direct and alveolar macrophage-associated routes. *Arch Toxicol* 2009;**83** 585
(5):429-437. 586
17. Choi HS, Ashitake Y, Lee JH, Kim SH, Matsui A, Insin N, et al. Rapid 587
translocation of nanoparticles from the lung airspaces to the body. *Nat* 588
Biotechnol 2010;**28**(12):1300-1303. 589
18. Haque S, Boyd BJ, McIntosh M, Pouton C, Kaminskas LM, Whittaker 590
MR. Suggested procedures for the reproducible synthesis of Poly(D,L- 591
lactide-co-glycolide) nanoparticles using the emulsification solvent 592
diffusion platform. *Current Nanoscience* 2018;**14**:1-6. 593
19. Boyd BJ, Kaminskas LM, Karellas P, Krippner G, Lessene R, Porter CJ. 594
Cationic poly-L-lysine dendrimers: pharmacokinetics, biodistribution, 595

AUTHOR QUERY FORM

 ELSEVIER	Journal: NANO	Please e-mail your responses and any corrections to:
	Article Number: 102291	E-mail: Corrections.ESCH@elsevier.spitech.com

Dear Author,

Please check your proof carefully and mark all corrections at the appropriate place in the proof (e.g., by using on-screen annotation in the PDF file) or compile them in a separate list. Note: if you opt to annotate the file with software other than Adobe Reader then please also highlight the appropriate place in the PDF file. To ensure fast publication of your paper please return your corrections within 48 hours.

For correction or revision of any artwork, please consult <http://www.elsevier.com/artworkinstructions>.

We were unable to process your file(s) fully electronically and have proceeded by

Scanning (parts of) your article
 Rekeying (parts of) your article
 Scanning the artwork

Any queries or remarks that have arisen during the processing of your manuscript are listed below and highlighted by flags in the proof. Click on the 'Q' link to go to the location in the proof.

Location in article	Query / Remark: click on the Q link to go Please insert your reply or correction at the corresponding line in the proof
Q1	Your article is registered as a regular item and is being processed for inclusion in a regular issue of the journal. If this is NOT correct and your article belongs to a Special Issue/Collection please contact s.sudhakar@elsevier.com immediately prior to returning your corrections.
Q2	The author names have been tagged as given names and surnames (surnames are highlighted in teal color). Please confirm if they have been identified correctly.
Q3	Supplementary caption was not provided. Please check the suggested data if appropriate, and correct if necessary.
Q4	Correctly acknowledging the primary funders and grant IDs of your research is important to ensure compliance with funder policies. We could not find any acknowledgement of funding sources in your text. Is this correct?
Q5	Ref. 33 is the same as Ref. 25. Can an alternative reference be provided to avoid repetition? If not, please delete the duplicate reference and renumber subsequent references. <div style="border: 1px solid black; padding: 5px; width: fit-content; margin: 0 auto;"> Please check this box if you have no corrections to make to the PDF file. <input type="checkbox"/> </div>

Thank you for your assistance.